optica

Temporal cloaking for data suppression and retrieval

Joseph M. Lukens,† Andrew J. Metcalf,† Daniel E. Leaird, and Andrew M. Weiner*

School of Electrical and Computer Engineering, Purdue University, West Lafayette, Indiana 47907, USA

**Corresponding author: amw@purdue.edu*

Received 12 September 2014; accepted 8 October 2014 (Doc. ID 222940); published 25 November 2014

Recent research on time cloaking has revealed a fascinating approach to hide temporal events from an interrogating optical field, by opening up and subsequently closing intensity gaps in a probe beam. Experiments thus far have demonstrated temporal cloaking of nonlinear interactions and high-speed optical data. Here we report a temporal cloak with the new capability not only to hide optical data, but also to concurrently transmit it along another wavelength channel for subsequent readout, masking the information from one observer while directing it to another. Additionally, the cloak succeeds in passing modulated data unscathed through a scrambling event, providing a new form of tampering resistance. Both examples launch a paradigm shift in temporal cloaking: instead of using time cloaks primarily to disrupt communication, we show how they can also improve data transmission, in turn greatly widening the range of possible applications in telecommunications.

OCIS codes: (060.0060) Fiber optics and optical communications; (070.6760) Talbot and self-imaging effects; (230.3205) Invisibility cloaks.

http://dx.doi.org/10.1364/OPTICA.1.000372

First proposed by McCall *et al.* [1], temporal cloaking is based on the transformation-optics formalism originally established for metamaterial spatial cloaks [2–4]. By elevating time to equal footing with three-dimensional space, space–time cloaks that hide regions of space over particular windows of time can be envisaged [1,5–8]. And although a full space–time cloak has yet to be realized, previous work [9,10] has indeed shown pure temporal cloaking for spatially single-mode light. (In another recent experiment [11], polarization self-trapping and scrambling was used to transmit or hide data from a continuous-wave probe. This approach represents a distinct form of cloaking in which polarization is manipulated rather than space or time, and for the purposes of this work, we limit ourselves to cloaking that truly generates and closes temporal intensity gaps.) These experiments clearly exhibited the salient feature of a temporal cloak: the ability to hide the presence of some event from a probe that without the cloak would have been significantly modified. Accordingly, the event is effectively erased from the "history" recorded by the probe field [1,6]. Yet one naturally could desire a more shrewd arrangement in which the event, while hidden from one optical beam, is perfectly visible to another probe, granting a desired recipient access to the history while cloaking it from an adversary. Such a feature is particularly suitable for optical communications, where the "histories" are streams of digital data that one may wish to secretly send to a distant party. Another restriction of the previous temporal cloaks is the limitation to continuous-wave input probe fields. Indeed, such fields do represent excellent test cases; possessing constant intensity over all time, they have no natural gaps in which events could take place and thus must be carefully manipulated to produce and close temporal holes. But of course it would be profitable to explore cloaking potential with noncontinuous-wave inputs as well, both to examine the limits of current arrangements and to explore possibilities for enhanced capabilities.

Our experiments address both of the previously mentioned shortcomings. First, we demonstrate a multiwavelength—or wavelength-division-multiplexed (WDM)—cloak in which optical data are hidden from the probe at one of the input frequencies but accurately transmitted along another wavelength. Second, we consider noncontinuous-wave input fields, which consist of pseudorandom modulation, obtaining faithful data transmission even when subjected to high-speed interference from the event; in this fashion, the cloak furnishes anti-tampering capabilities, removing the impact of destructive modulation. These additions herald a fundamental change in how such cloaks can be viewed, for whereas previous time cloaks only *prevented* an observer from discovering the event, our new implementation reveals how time cloaks can be exploited to selectively *transmit* data as well. Considering the practical view that the most probable long-term applications of temporal cloaks will focus on improving current communication systems (e.g., as in [12]) rather than disrupting them, our results represent a key step forward.

The previous demonstrations of temporal cloaking [9,10] were developed by drawing on the concept of space–time duality [13–16], the mathematical correspondence between two common approximations to the wave equation: narrowband dispersion and paraxial diffraction. In particular, a central component of the second cloak [10] was the temporal Talbot effect [17]—the analogue of spatial Talbot self-imaging [18,19]—which exploits temporal interference to generate intensity gaps. Through a combination of phase modulation and dispersion originally considered in frequency-comb generation [20–23], this cloak implemented Talbot self-imaging and time lensing to convert a continuous-wave input into a high-repetition-rate train of pulses with wide regions of zero intensity, wherein any events would escape detection. Then by traversing the opposite values of dispersion and complementary phase modulation, the pulse train was converted back into the original continuous-wave beam, ideally with no evidence of its detour as high-extinction pulses. In transitioning toward a multiwavelength cloak, we once again invoke space–time duality by drawing on a variation of Talbot interference, the so-called Lau effect [18,24,25]. Whereas the basic Talbot phenomenon requires a spatially coherent beam, the Lau effect considers instead a spatially incoherent source illuminating two gratings. Narrow slits on the first grating create a series of individually coherent but mutually incoherent line sources, and each of these sources then generates a Talbot carpet after the second grating, all of which sum incoherently to give a total intensity that can correspond to a high-contrast image if the patterns are spatially aligned [18].

A temporal analogue of the Lau effect [26,27] has been considered experimentally for optical fields consisting of mutually incoherent narrowband lasers manipulated by an electro-optic modulator [28]. By tuning the laser frequency spacing, the delay between corresponding output time-domain waveforms can be adjusted to any amount within a period, from complete temporal coincidence to a half-period delay. And such delay control of temporal Talbot imaging is precisely what we require for a multiwavelength time cloak. Individually, with no event present, each input wavelength should propagate through the cloak modulators and dispersion and emerge at the output as a continuous-wave signal; however, when an event is applied in the form of data modulation, one wavelength should escape without modulation, whereas the second should contain a faithful reproduction of the event data. To achieve this, we make use of the Lau effect and choose the wavelength separation so that both lasers yield compressed pulse trains that are delayed by one half-period relative to each other at the event modulator, ensuring that the data impact only one of the two wavelength channels. Plots in Fig. 1(a) provide cartoons of the pulse trains derived from each input frequency at various stages in the circuit, showing the overlap and interleaving necessary for our multiwavelength cloak. (See Supplement 1 for details on these design conditions).

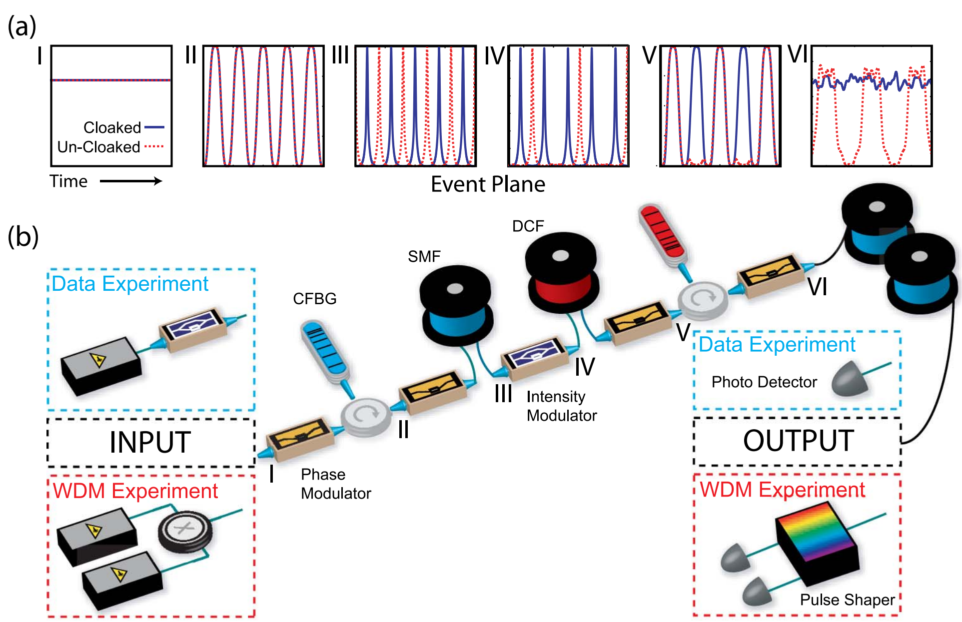

Fig. 1. Basic outline of temporal cloak. (a) Waveform progression for multiwavelength cloak. Blue and red lines denote the intensity in the channels to be cloaked and to receive the data, respectively. Roman numerals represent various points in the circuit: I, input to first phase modulator; II, after quarter-Talbot dispersion; III, at event plane just prior to event modulation; IV, at event plane immediately after modulation; V, before compensating quarter-Talbot dispersion; VI, at output. Only the red channel is impacted by the data modulation, which is an alternating zero–one sequence in this example. (b) Experimental setup. Boxes at the input and output show differences between the multiwavelength cloak ("WDM Experiment") and data-as-input cloak ("Data Experiment"). Blue fibers and Bragg gratings signify anomalous dispersion, whereas red represents normal dispersion. CFBG, chirped fiber Bragg grating; SMF, single-mode fiber; DCF, dispersion-compensating fiber.

Figure 1(b) offers a schematic of the experimental setup, with the boxes labeled "WDM experiment" marking the input and output configurations for multiwavelength cloaking. We couple two independent monochromatic lasers into the cloaking circuit, one of whose wavelengths is tunable, and we propagate them through a combination of phase modulation and dispersion that converts them into interleaved pulse trains at the event plane. The event consists of intensity-modulated pseudorandom data, which ideally impacts only one of the two trains, and after reconstruction the two wavelength channels are demultiplexed with a pulse shaper [29,30] and then detected. As in [10], the extra dispersive fiber after the fourth phase modulator is added to achieve approximately zero net dispersion between the event and detector, so that turning the phase modulators off allows the event data to appear at the output without distortion. Moreover, when the cloak is operating, it is important to note that the amplitude of fluctuations in the output depends not only on the power in residual spectral sidebands, but also on the phase, as this determines whether contributions at the same radio frequency will add constructively or cancel each other out. Accordingly, we run all modulators at 12.11 GHz, rather than the 12.5 GHz estimated for ideal Talbot self-imaging, since we found in simulation that this frequency gives slightly improved performance for our combination of dispersive elements. A more detailed description of the experimental methods is provided in Supplement 1.

The measured spectrum when only the first two phase modulators are running is given in Fig. 2(a), with two distinct flat-top combs generated about each carrier frequency. The broad bandwidth indicates that both combs will support short pulses at the event plane. To introduce the event, we apply inverted return-to-zero data to the intensity modulator; when all phase modulators are off, both wavelength channels retain this data at the output, as evidenced by Fig. 2(b). However, turning on the cloak allows us to hide the data from one wavelength while continuing to broadcast it along the other; Fig. 2(c) gives the received signals when the phase modulators are on and optimized to cloak the short-wavelength channel. While the originally strong data modulation is removed on the output of the short-wavelength filter, the long-wavelength channel maintains high-contrast modulation. The received data have been converted to a nonreturn-to-zero format—which is as expected from theory due to the modulation and dispersion subsequent to the intensity modulator—but clear transitions between 0 and 1 certify that the digital stream is fully maintained. Moreover, by shifting the event modulator's timing half a period, the roles of each channel can be reversed; as illustrated in Fig. 2(d), in this case the long-wavelength channel is now cloaked, with the short wavelength picking up the data.

Alternatively, instead of taking the event to represent the information-bearing quantity of interest—either to be hidden from or transmitted to another party—one may view the event as unwanted modulation that corrupts the input field; in this perspective, the cloak becomes a data *preserver* rather than a data *concealer*. Accordingly, it is profitable to consider data-modulated inputs rather than just continuous-wave fields, which naturally lack any temporal information. At first glance, since the cloak is constructed assuming a single-frequency probe, it may appear that our design is inherently ill-suited for accepting a time-varying input. But the cloak itself operates at a high speed, so the requirement of constant intensity in effect means only that the input bandwidth be much smaller than the cloak repetition rate ω_{rep}, or equivalently that the input field intensity must remain roughly constant over several clock periods. This intuitive picture implies that the cloak should still perform well with a data signal at the input, provided that the data rate is sufficiently lower than ω_{rep}.

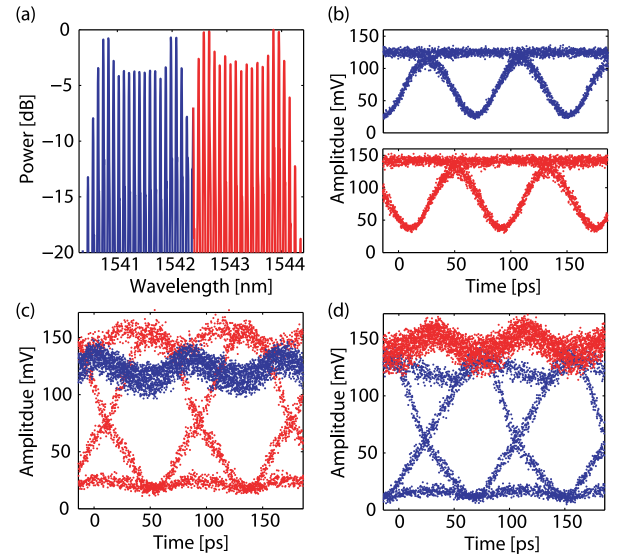

Fig. 2. Experimental results for multiwavelength cloak. (a) Optical spectrum when the first two phase modulators are running. Colors indicate from which input laser a given spectral line was primarily generated, with blue representing the short-wavelength laser and red the long-wavelength one. (b) Received output for the short-wavelength (blue) and long-wavelength (red) demultiplexed channels when the event modulator is running and all phase modulators are off. (c) Received signals when the cloak is on and optimized to cloak the blue channel but transmit along the red. (d) Corresponding waveforms when the cloak is instead aligned to transmit data on the blue channel and cloak the red.

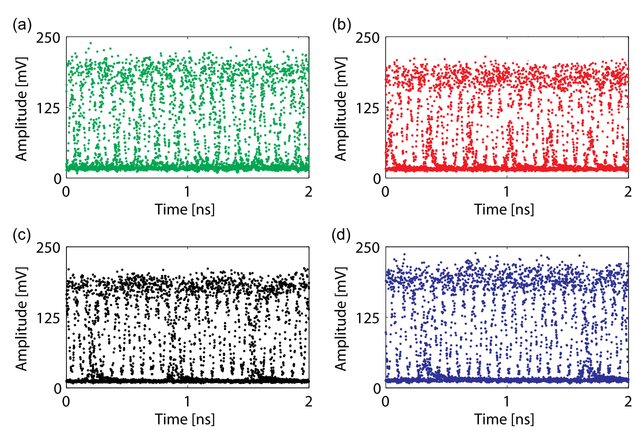

Fig. 3. Received signals for data-as-input experiment, when the cloak is off. (a) Input data rate is two times less than the clock. (b) Four times. (c) Eight times. (d) Sixteen times. In all cases, the high-speed event modulation at 12.11 GHz significantly corrupts the input data.

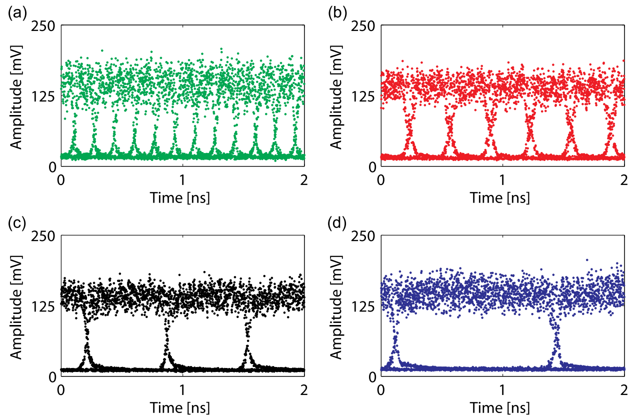

Fig. 4. Received signals for data-as-input experiment, when the cloak is on. (a) Input data rate is two times less than the clock. (b) Four times. (c) Eight times. (d) Sixteen times. Now the input sequences are fully recovered, with clear data signals observed at the appropriate repetition rates.

We examine this idea experimentally with the setup of Fig. 1(b), but now using the transmitter and receiver in the "Data Experiment" insets. A single continuous-wave laser is modulated at some fraction of the clock frequency with nonreturn-to-zero data; explicitly, we consider clock-division factors of 2, 4, 8, and 16, corresponding to input data rates of 6.06 Gb/s, 3.03 Gb/s, 1.51 Gb/s, and 757 Mb/s, respectively. When the phase modulators are off, the high-speed event completely destroys the input data sequence; as illustrated in Fig. 3, the input data are nearly impossible to observe, corrupted by the fast modulation. Yet when the cloak is turned on, the input field is guided around this distorting modulation and recovered at the output, as indicated by the results in Fig. 4. For all input repetition rates, clear data at the correct period are now seen, with the event's impact reduced to residual noise at the high voltage level. This noise is strongest in the divide-by-two case, which makes sense, as the data rate is highest here and thus most removed from the continuous-wave ideal. Moreover, numerical simulations indicate only marginal performance improvement for data rates below the divide-by-eight case, which is qualitatively confirmed by the lack of significant noise reduction between Figs. 4(c) and 4(d). (There are also several paths for future cloak enhancements; for further discussion, refer to Supplement 1).

In summary, we have demonstrated two new uses for temporal cloaking in high-speed telecommunications. The first, a multiwavelength cloak, allows data that are hidden from one wavelength channel to be transmitted along an alternative one; in the second, a corrupting event is cloaked from an input digital message, thereby allowing faithful transmission of the incoming data past an aggressive modulation signal. Both realizations offer new perspectives on temporal cloaking for improving data communication systems rather than disturbing them. It will be interesting to explore how this two-sided nature of time cloaking may be exploited in future developments in this field, whether in the exotic quest for a full space–time cloak or in more mundane—but no less important—efforts to improve optical communications.

FUNDING INFORMATION

Naval Postgraduate School (N00244-09-1-0068); U.S. Department of Defense (DOD) (NDSEG Fellowship).

ACKNOWLEDGMENT

We thank V. Torres-Company for discussions on the Lau effect.

†These authors contributed equally to this work.

See Supplement 1 for supporting content.

REFERENCES

1. M. W. McCall, A. Favaro, P. Kinsler, and A. Boardman, J. Opt. **13**, 024003 (2011).
2. U. Leonhardt, Science **312**, 1777 (2006).
3. J. B. Pendry, D. Schurig, and D. R. Smith, Science **312**, 1780 (2006).
4. H. Chen, C. T. Chan, and P. Sheng, Nat. Mater. **9**, 387 (2010).
5. R. B. Li, L. Deng, E. W. Hagley, J. C. Bienfang, M. G. Payne, and M.-L. Ge, Phys. Rev. A **87**, 023839 (2013).
6. P. Kinsler and M. W. McCall, Ann. Phys. **526**, 51 (2014).
7. P. Kinsler and M. W. McCall, Phys. Rev. A **89**, 063818 (2014).
8. I. Chremmos, Opt. Lett. **39**, 4611 (2014).
9. M. Fridman, A. Farsi, Y. Okawachi, and A. L. Gaeta, Nature **481**, 62 (2012).
10. J. M. Lukens, D. E. Leaird, and A. M. Weiner, Nature **498**, 205 (2013).
11. P. Y. Bony, M. Guasoni, P. Morin, D. Sugny, A. Picozzi, H. R. Jauslin, S. Pitois, and J. Fatome, Nat. Commun. **5**, 4678 (2014).
12. S. Arnon and M. Fridman, J. Lightwave Technol. **30**, 3427 (2012).
13. B. H. Kolner and M. Nazarathy, Opt. Lett. **14**, 630 (1989).
14. B. H. Kolner, IEEE J. Quantum Electron. **30**, 1951 (1994).
15. V. Torres-Company, J. Lancis, and P. Andrés, in *Progress in Optics* (Elsevier, 2011), Vol. **56**, Chap. 1.
16. R. Salem, M. A. Foster, and A. L. Gaeta, Adv. Opt. Photon. **5**, 274 (2013).
17. T. Jannson and J. Jannson, J. Opt. Soc. Am. **71**, 1373 (1981).
18. K. Patorski, in *Progress in Optics* (Elsevier, 1989), Vol. **27**, Chap. 1.
19. J. Wen, Y. Zhang, and M. Xiao, Adv. Opt. Photon. **5**, 83 (2013).
20. T. Komukai, T. Yamamoto, and S. Kawanishi, IEEE Photon. Technol. Lett. **17**, 1746 (2005).
21. V. Torres-Company, J. Lancis, and P. Andrés, Opt. Express **14**, 3171 (2006).
22. V. Torres-Company, J. Lancis, and P. Andrés, Opt. Lett. **33**, 1822 (2008).
23. A. J. Metcalf, V. Torres-Company, D. E. Leaird, and A. M. Weiner, IEEE J. Sel. Top. Quantum Electron. **19**, 3500306 (2013).
24. E. Lau, Ann. Phys. **437**, 417 (1948).
25. J. Jahns and A. W. Lohmann, Opt. Commun. **28**, 263 (1979).
26. D. Zalvidea, R. Duchowicz, and E. E. Sicre, Appl. Opt. **43**, 3005 (2004).
27. J. Lancis, C. M. Gómez-Sarabia, J. Ojeda-Castañeda, C. R. Fernández-Pousa, and P. Andrés, J. Eur. Opt. Soc. Rapid Pub. **1**, 06018 (2006).
28. V. Torres-Company, C. R. Fernández-Pousa, and L. R. Chen, Opt. Lett. **34**, 1885 (2009).
29. A. M. Weiner, Rev. Sci. Instrum. **71**, 1929 (2000).
30. A. M. Weiner, Opt. Commun. **284**, 3669 (2011).